Electrochemical reduction of indium and tin from ITO

Bo Qin[1], Ana Maria Martinez[2], Ragnhild E. Aune[1], Geir Martin Haarberg[1]

[1] Department of Materials Science and Engineering,
Norwegian University of Science and Technology, NTNU, NO-7491, Trondheim, Norway
2 SINTEF Materials and Chemistry, NO-7465 Trondheim, Norway

Abstract
The electrochemical behaviour of ITO (indium oxide combined with 10 percent tin oxide) was studied in molten LiCl-KCl at 450 °C. The direct de-oxidation of ITO were investigated by using different electrodes such as Mo wire and liquid zinc. An ITO covered glass electrode has been investigated by electrochemical means in molten LiCl-KCl at 450 °C using Mo wire current collector. The findings, together with SEM and EDX analyses, confirmed ITO layer has been reduced.

Keywords
ITO, electrochemical reduction, molten salt

1. Introduction
Indium is a rare metal. The largest end use for indium is in ITO thin-film coatings, which represent approximately 72 % of the indium market [1]. ITO has strong properties of electrical conductivity, heat reflection, and transparency. ITO can be spread as thin film on glass or plastic to act as a transparent electrical conductor and infrared reflector. However, indium has recycling rates less than 1 % [2]. Various methods for recycling of indium from secondary sources containing indium, in particular ITO sputtering waste have been reported. The growth of the application augmented the requirement for high grade purity of indium and the low recycling rates inspired the study of new indium electrorefining processes in fused salt media. High temperature molten salts play important roles in modern electrochemical research and industrial practices. Electrochemical deoxygenation of some metals was investigated. In molten CaC12, removal of oxygen from yttrium [3], the removal of oxygen from rare-earth metals [4], and the removal of oxygen in titanium [5] were achieved.

In the last decade, a new electrochemical process has been developed in order to convert solid oxides into their metal: the direct electrochemical reduction. Chen et.al have first achieved the direct reduction of TiO_2 into Ti in a molten chloride salt composed of $CaCl_2$ which is now known as the FFC Cambridge process [6]. The overall reaction is the oxygen removal from a solid M_xO_y oxide at the cathode (a) and the formation of CO_2 (g) at the carbon anode (b), according to:

$$M_xO_y\,(s) + 2ye^- = xM\,(s) + yO^{2-} \qquad (a)$$

$$2O^{2-} + C(s) = CO_2\,(g) + 4e^- \qquad (b)$$

The process could proceed by oxygen ionization without the need for depositing calcium. The oxygen ions become free to leave the cathode, to diffuse in the electrolyte, and to discharge at the anode. The advantages of the electrochemical reduction process are as follows. The reduction and electrowinning steps are performed simultaneously. The oxide ion concentration in the salt is almost constant and can be maintained at a low value. The amount of salt used in

the process maybe small because oxide ions don't accumulate in the salt bath [7]. The simple electrochemical process attracted worldwide attention and significant efforts have been made since then to study and develop the process for production of many metals/alloys from their oxides, for example, electrochemical reduction of ZrO_2 [8], HfO_2 and niobia-doped HfO_2 [9], CeO_2 [10], V_2O_5 [11], Cr_2O_3 [12], UO_2 [13], Fe_2O_3 [14], Ta_2O_5 [15], UO_2-PuO_2 mixed oxides [16], Al_2O_3 [17], SiO_2 [18, 19], WO_2 [20] and the production of Ti–Mo alloys [21], Ti-W alloys [22], TiFe Alloys [23], NiTi [24], NbSi alloys [25] and so on.

No data are available in the literature for the electrochemical reduction of ITO, and SnO_2 has been studied only a little in Li-NaF-Li_2O(1 mass.%) [26]. The electrochemical reduction of ITO was investigated in the present work using different working electrodes.

2. Experimental

The furnace was a vertical tube furnace controlled by at Eurotherm 902 controller. The electrolyte LiCl: KCl with the eutectic composition (58.2: 41.8 mol%) was contained in a cylindrical alumina crucible and was situated inside a gas-tight quartz container. At the top of the quartz tube a clamp fitted with 3 rubber O-rings ensured an air-tight assembly between the tube itself and the lid of the tube. The experiments were performed under inert argon atmosphere. To minimize the temperature gradient, a total of 4 evenly spaced alumina radiation shields extended from the crucible up to the top of the tube. The temperature in the cell was controlled with a Pt 10% Rh vs Pt thermocouple. The reference electrode in this thesis was a silver wire dipped in LiCl-KCl melt containing 0.75mol kg-1 AgCl and placed in the mullite. The electrochemical studies were performed using a graphite rod (8mm) as a counter-electrode. The voltammetry studies were performed with a Zahner pp201 computer controlled potentiostat. The cathode deposits were examined with a scanning electron microscope (SEM) Hitachi S3400N LV-SEM equipped with an energy dispersive spectrometer(EDS) probe Oxford instruments INCA 7021. Molybdenum wire and zinc liquid were used as working electrodes in this study see Fig.1. In Fig. 1 (a), ITO pellets connected with a Mo wire were used as the cathode. In Fig.1 (b), high purity zinc was placed at the bottom of the alumina tube. ITO pellets were placed on the top of the zinc metal. Electrons are supplied from the Mo wire to the Zn metal. There is a hole on the alumina tube to make the molten salt flow in. If ITO was reduced to metallic In or Sn, In-Sn alloy will sink to the bottom of the crucible to alloy with Zn. In Fig.1 (c), a molybdenum wire is wound around the ITO glass (one side of the glass coated by ITO) which supplies electrons to a selected region of the ITO film. This electrode was used for cyclic voltammetry and bulk reduction experiments. This study will discuss the experiments according to different working electrodes.

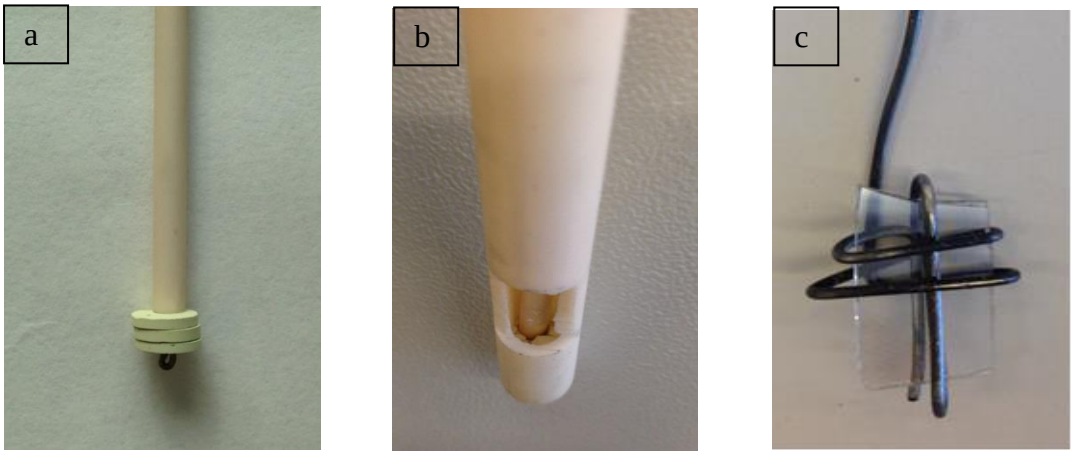

Fig.1 Photos of the oxide working electrode (a), Zn working electrode (b) and Mo contacting electrode (c)

3. Thermodynamics

ΔG^{θ} is equal and opposite to the electrical potential generated and is expressed by the following equation

$$\Delta G^{\theta} = - nE^{\theta}F \quad (1)$$

where 'n' refers to the number of electrons participating in the reaction, 'E^{θ}' is the standard electromotive force (EMF) and 'F' is the Faraday constant.

All spontaneous reactions occur with a decrease in the Gibbs energy, while the driving force change of all decomposition reactions in these experiments ΔG is increased. Thus, they are nonspontaneous. The standard EMF is negative, so energy has to be supplied from an external source. The magnitude of the EMF also depends upon the temperature and the activities of the solute species. This is taken into account by the Nernst equation:

$$E = E^{\theta} - RT/(nF) \cdot \ln K \quad (2)$$

where: R universal gas constant ($8.314 J \bullet K^{-1} \bullet mol^{-1}$)
T absolute temperature (K)
n number of electrons transferred in the reaction
F Faraday constant ($96485 J \bullet V^{-1} \bullet mol^{-1}$)
K equilibrium constant
So decomposition voltages for different reactions can be derived according to Temkin model[27]. Here a_{Metal} and a_{gas} can be regarded as 1. Table 1 shows the standard electrode potentials E^{θ} and theoretical electrode potentials E for different electrode systems obtained in mole fraction scale versus the potential of Ag^{+}/Ag reference electrode and also standard decomposition voltages of oxides. The calculations were performed from the known thermodynamic data at 723 K using HSC Chemistry 6.1 [28].

Table 1 Standard electrode potentials E^{θ} and theoretical electrode potentials E at 450 ℃

Couple/Reaction	E^{θ}/V	E/V
K(I)/K	-2.90	-2.70
Li(I)/Li	-2.71	-2.51
Ag(I)/Ag	0.00	0.00
Cl_2/Cl-	0.91	1.11
$In_2O_3 = 2In + 1.5O_2(g)$	-1.19	
$In_2O_3 + 1.5C = 2In + 1.5CO_2(g)$	-0.16	
$SnO_2=Sn+O_2(g)$	-1.12	
$SnO_2+C=Sn+CO_2(g)$	-0.09	
$SnO=Sn+0.5O_2(g)$	-1.08	
$SnO + 0.5C = Sn + 0.5CO_2(g)$	-0.06	

The aim of the present paper is to recover In and Sn in the same molten alkali electrolyte. Indeed, indium easily forms alloys with other melts such as tin as illustrated in the binary phase

diagram of In-Sn presented in Fig. 2 [29]. The In-rich and Sn-rich parts of the phase diagram include peritectic reactions. In and Sn form a complete miscible liquid mixture at 723 K. The alloys containing 11-15 at% Sn are mixtures of the In-rich phase (In) and β phases while alloys below 11 at% Sn or over 15 at% Sn are In-rich phase (In) or β single phase solid solutions at room temperature, respectively [30]. The atomic percent of tin in ITO is no more than 10%, so the alloy is In-rich phase (In) single phase.

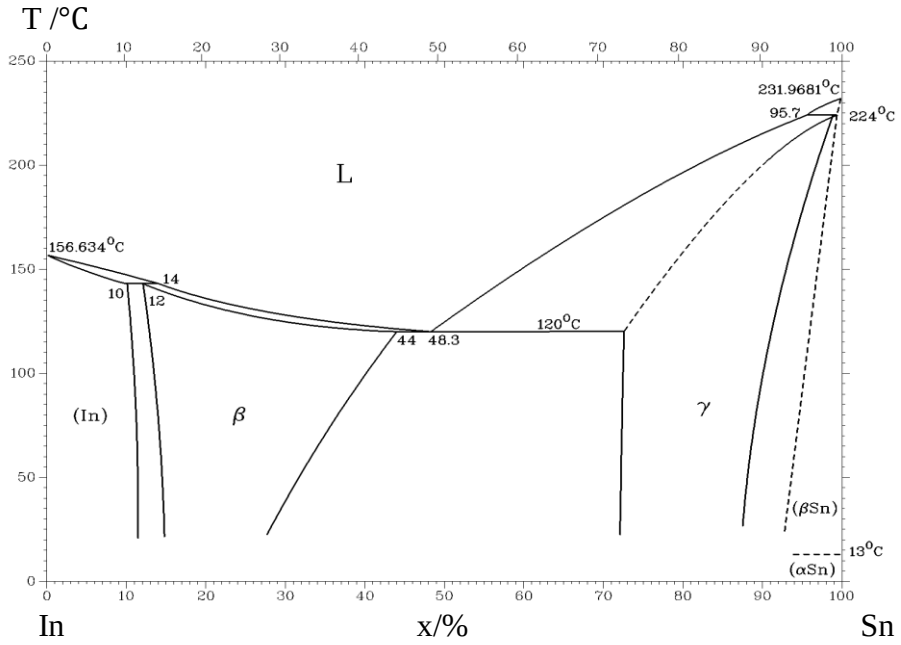

Fig. 2 The In-Sn equilibrium binary phase diagram

4. Results and discussion

4.1 Electrochemical behavior of indium and tin chlorides

For comparison, cyclic voltammogram related to the reduction of $InCl_3$ and $SnCl_2$ ($mInCl_3$:$mSnCl_2$=10:1) in the fused LiCl-KCl at 450°C was obtained in Fig. 3. During the reduction scan, several peaks have been observed. Peaks B, C probably correspond to the reduction of In^{3+} to In^{+}, metallic tin deposition, respectively. Sn will deposit first and then In will incorporate in the Sn giving a liquid alloy. This probably corresponds to peak D. In accordance with the negative sweep, the positive sweep of the cyclic voltammogram comprises the features D', C' and B'. They are associated with the reverse reactions to those mentioned above, the dissolution of alloy, the dissolution of tin and the oxidation of In^{+} to In^{3+}. The peak couple A'/A attribute to the Sn^{2+}/Sn^{4+} redox couple.

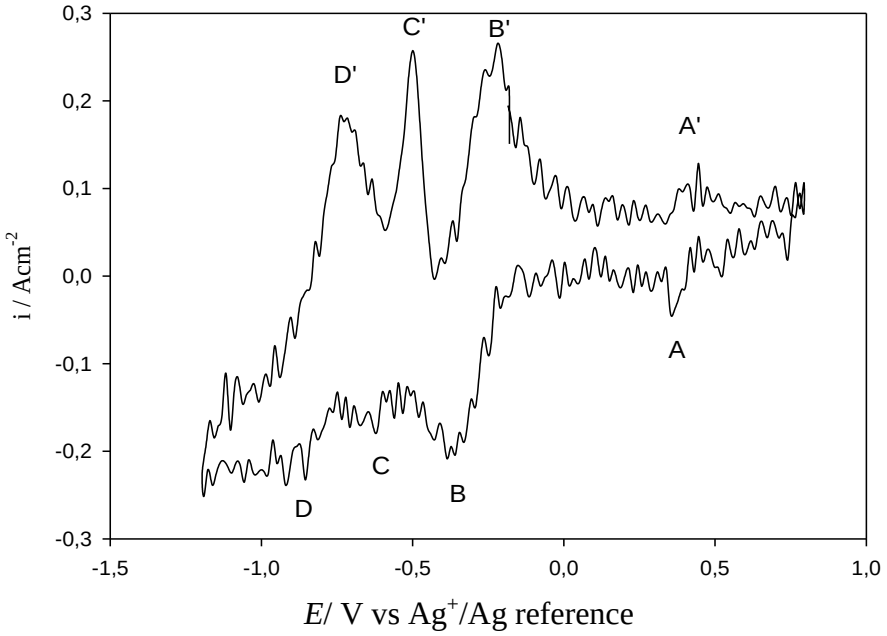

Fig. 3 Cyclic voltammogram obtained related to the reduction of $InCl_3$ and $SnCl_2$ (m_{InCl3}:m_{SnCl2}=10:1) in the fused LiCl-KCl at 450℃. Sweep rates: 1v/s. The potential is swept in the cathodic direction from the open circuit potential.

4.2 Electrochemical behaviour of ITO-Molybdenum wire working electrode

According to the phase diagram of the In–Mo system [31], there is no intermetallic compound phase in the equilibrium phase. The solubility of In in Mo is negligible at temperature lower than 1000 ℃. So Mo is 100% inert with respect to In at the working temperature. Actually, Mo is suggested as an effective diffusion barrier against the attack of liquid tin by investigation of phase formation and reaction kinetics in the Mo–Sn system [32].

Fig. 4 shows the results of a voltammetric study of ITO deposition using a molybdenum rod working electrode. Only one reduction peak was observed and seems like the deposition of tin. Comparing with previous study [33], The main cathodic peak can be ascribed to the reduction of SnO_2 since the mole fraction of In_2O_3 is larger than SnO_2. Thus, a shoulder superimposed on the main cathodic peak can be assigned to the reduction of In_2O_3, of which the start reduction potential is more positive than that of SnO_2.

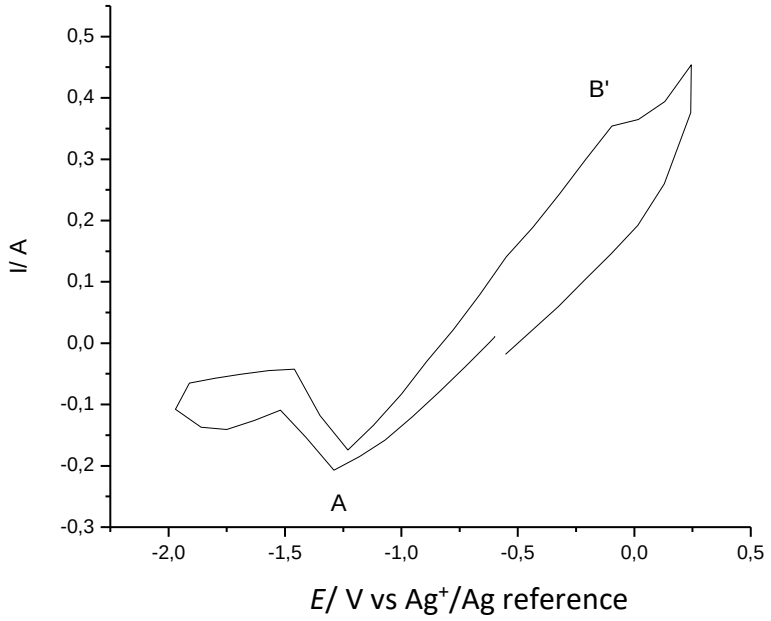

Fig. 4 CV of a Mo working electrode with ITO in molten LiCl-KCl at 450°C with a potential scan rate of 500mV/s. The potential is swept in the cathodic direction from the open circuit potential.

4.3 Electrochemical behaviour of ITO-Zn working electrode

Castrillejo et al. [34] concluded that the In(I)/In(O) couple must be more negative in potential than in Zn(II)/ Zn(0) couple, therefore Indium metal in contact with the melt reacts quantitatively to give zinc metal. In these experiments, in order to increase the area of the three phase boundary (cathode, oxide and molten salt), liquid zinc was tried as cathode. The phase diagrams of the In Zn [35] or Zn-Sn [36] system show that no existence of any intermetallic compounds. The direct deoxidization of ITO was investigated.

Potentiostatic electrolysis was conducted for the ITO at -1.7V (versus reference) for 2 h. Fig. 5 shows the current transient curve during the electrolysis. The cathodic current decreased about 300 mA during the first 10 min of the experiment, and after some fluctuation the current stabilized. After electrolysis of the ITO, the SEM of zinc matrix was shown in Fig. 6. A lot of indium and tin intensive areas were found from the EDS element distribution maps (Fig. 7). This purple area is indium-intensive and the yellow areas are tin. In the indium and tin intensive areas, little of zinc and oxygen exist. The atomic ratios of In, Sn, O and Zn in the indium and tin intensive areas are 82.8: 6.9: 7.5: 2.7(Fig.8). ITO was almost completely reduced.

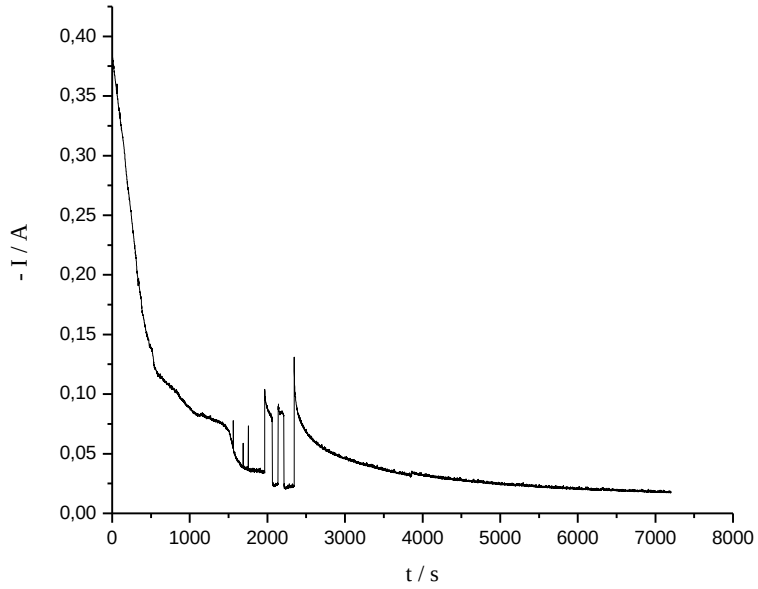

Fig.5 Current with time of ITO during constant potential electrolysis at -1.7 V for 2 h

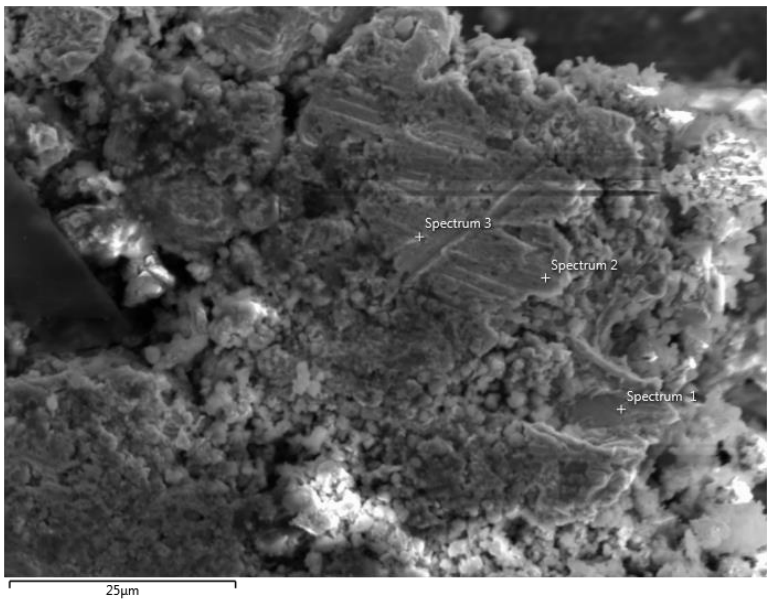

Fig. 6 The SEM of zinc matrix after ITO electrolysis

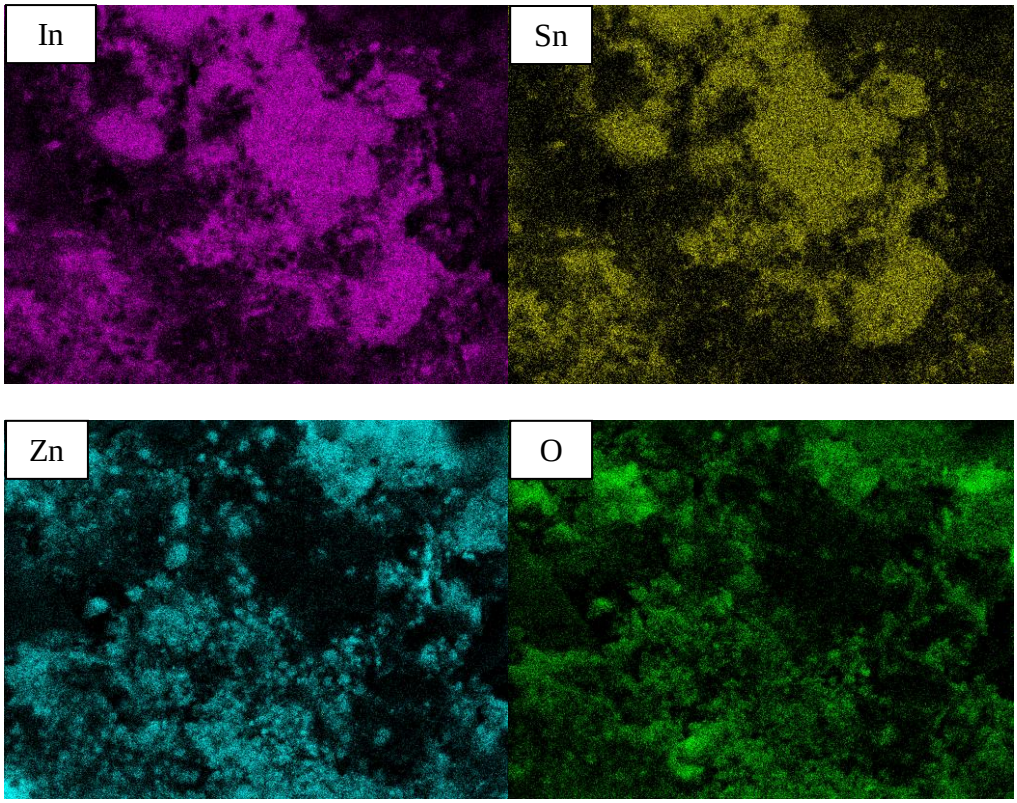

Fig. 7 EDS element distribution maps after ITO electrolysis

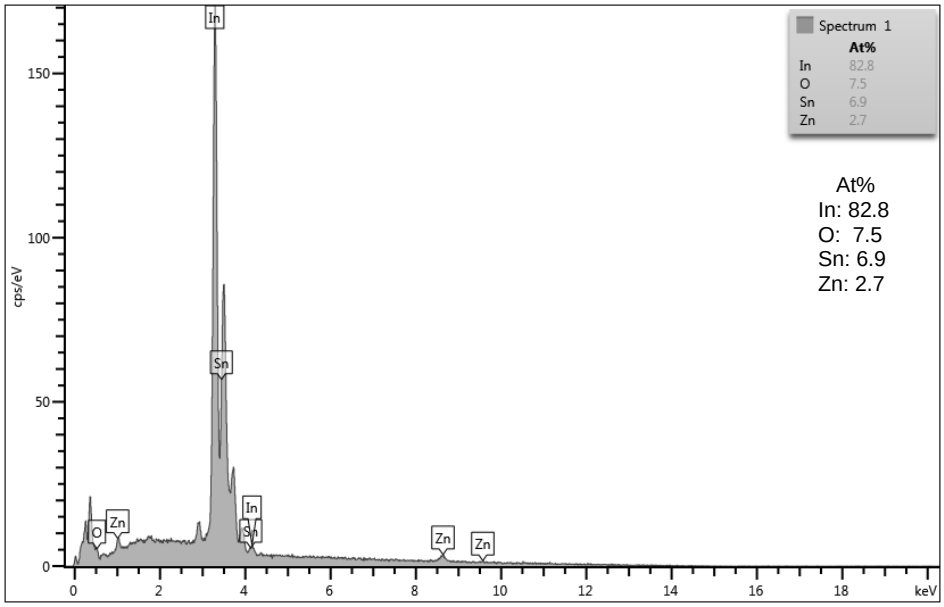

Fig. 8 EDS of the cathode deposit for point 1

4.4 Electrochemical reduction of indium and tin from ITO coated glass

Cyclic voltammetry was performed on ITO coated glass see Fig.9. By increasing the potential limit in the negative direction, two reduction peaks A and B were observed before the deposition of electrolyte C. Peak A was proposed to be for the reduction of In_2O_3 and SnO_2 which overlapped each other because of the close reduction potentials. Peak B may be attributed to the reduction of SiO_2 [18], because only a thin layer of ITO covered on the glass. D' probably corresponds to the anodic dissolution of the Mo wire [37].

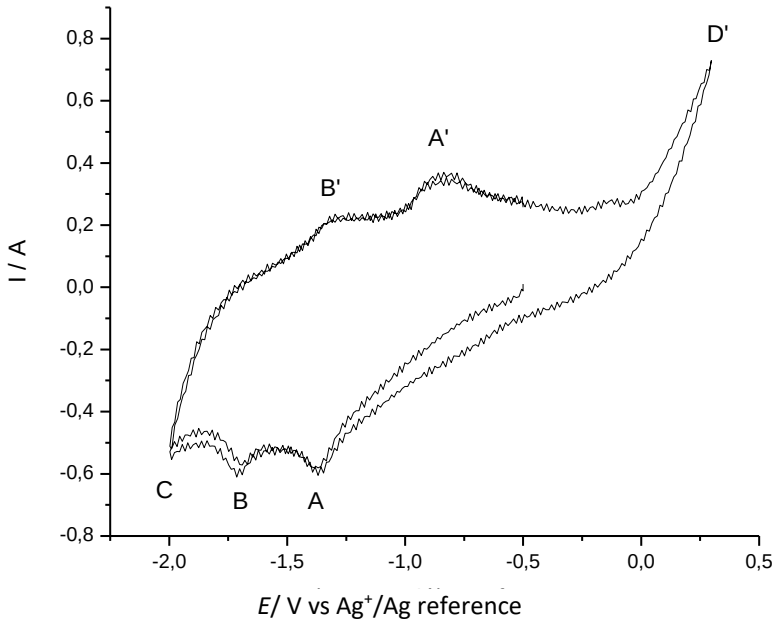

Fig. 9 CV of ITO coated glass with a potential scan rate of 1V/s

Fig. 10 shows the electrochemical response of a cell when -1.7 V constant potential difference was applied between a Mo wire cathode and the reference electrode. It shows the current decays with time.

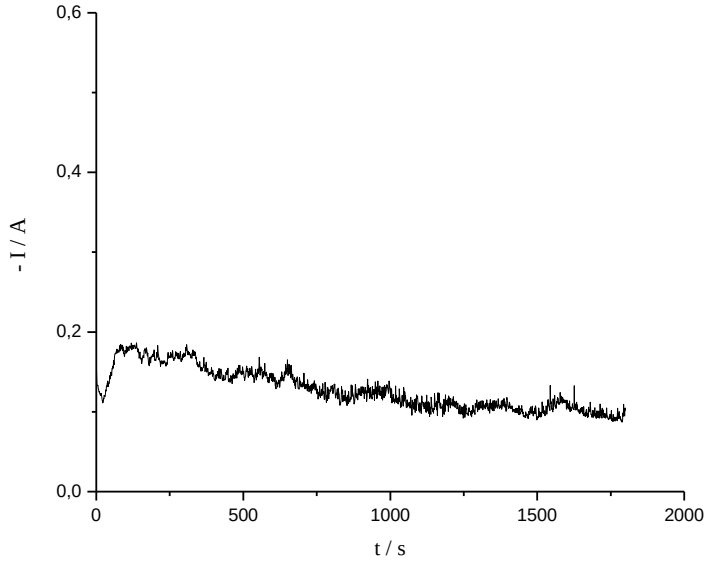

Fig. 10 Current with time of ITO coated glass during constant potential electrolysis

Fig. 11 shows a photograph of the specimens obtained by constant potential electrolysis at -1.7 V versus reference for 30 minutes. The molybdenum wire was removed and the sample was washed in the distilled water. It can be seen that after electrolysis some electrolytic reactions happened in the molybdenum wire contacted area and the colour turned black. Moreover, an obvious groove was also formed. The SEM image of the contacting region of the ITO covered glass electrolysed for 30 minutes was shown in Fig. 12. A vertical elemental analysis was scanned on the groove by EDS line element analysis which was shown in Fig. 13. We can see that all the element concentrations were decreased. The contents of In (purple line) and Sn (red line) are constant in the non-contacting region of ITO layer. But they could not be found in the reaction zone after the electrolysis. The concentrations of Si and O are also reduced significantly. This shows that the silicon is reduced at the applied voltage -1.7 V versus reference and the ITO layer was firstly reduced to liquid Sn and In (at 723 K), which mix with the electrolyte, and next, SiO_2 was also reduced to Si.

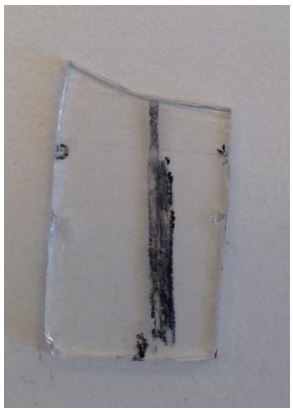

Fig. 11 Photograph of the contacting electrode after electrolysis

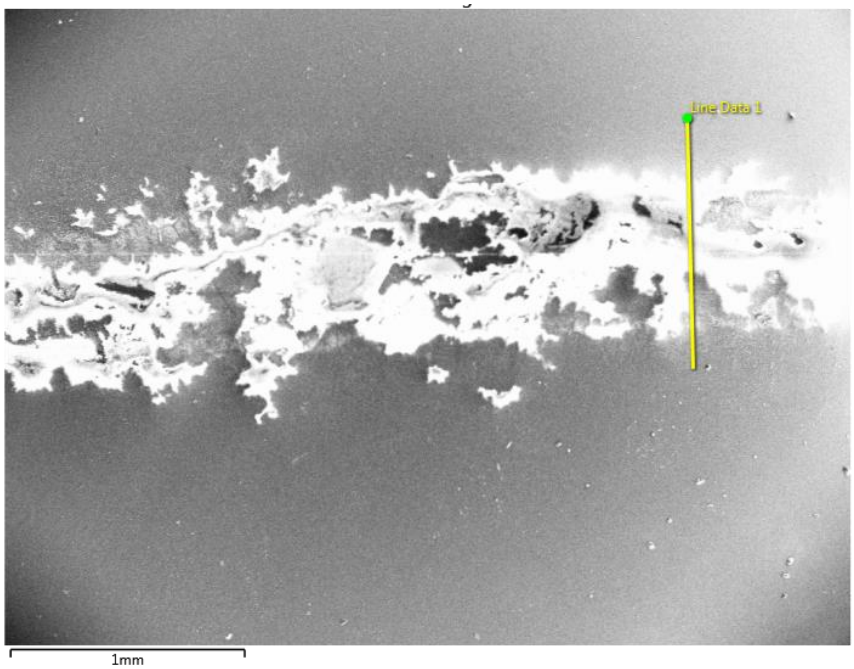

Fig. 12 SEM image of the contacting region of the ITO covered glass electrolysed for 30 minutes

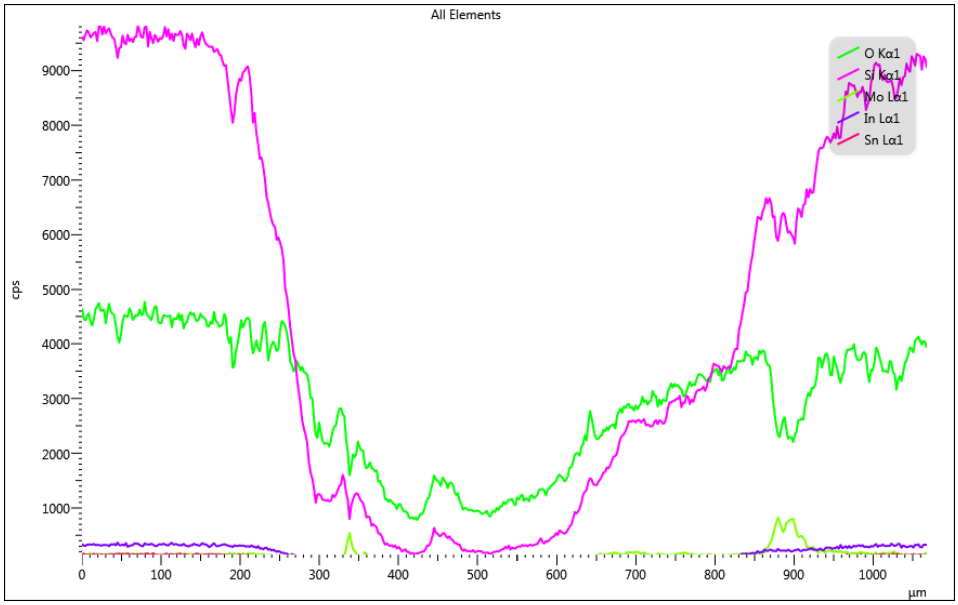

Fig. 13 EDS element line distribution maps for the contacting region

5.4 Conclusions

1. During the cathodic reduction and anodic oxidation scans of molten salt containing indium chloride and tin chloride, the redox couples In^{3+}/In^{+}, Sn^{4+}/Sn^{2+} and Sn^{2+}/Sn were observed. Sn will deposit first and then In will incorporate in the Sn giving a liquid alloy.
2. Only one reduction peak was observed in the cathodic scan for ITO which starts at -0.67 V when using Mo working electrode.
3. Liquid zinc was used as cathode taking into account the low melting points of indium and tin. Potentiostatic electrolysis was conducted for ITO at -1.7 V for 2 hours. ITO was almost completely reduced.
4. Electrochemical methods were applied for removing oxygen from ITO coated in a molten LiCl-KCl electrolyte using a Mo wire contacting electrode at 450 °C. The electrolytic reduction peak of ITO film occured at around -1.25 V. At a more negative potential -1.7 V SiO_2 was also reduced to Si.

The findings, together with SEM and EDX analyses, confirmed the ITO has been reduced. The results are promising for the aim of recycle In and Sn from ITO.

Acknowledgments

Financial support from the Department of Materials Science and Engineering of the Norwegian University of Science and Technology is gratefully acknowledged.

References

1. J.D.J.a.M.W. George, Indium. U.S. Geological Survey, (2004).
2. O.H. Ltd, Study into the feasibility of protecting and recovering critical raw materials through infrastructure development in the south east of England. European Pathway to Zero Waste, (2011).
3. T.H. Okabe, T.N. Deura, T. Oishi, K. Ono, and D.R. Sadoway, Electrochemical deoxidation of yttrium-oxygen solid solutions. Journal of Alloys and Compounds, **237**(1-2), p. 150-154 (1996).

4. K. Hirota, T.H. Okabe, F. Saito, Y. Waseda, and K.T. Jacob, Electrochemical deoxidation of RE-O (RE=Gd, Tb, Dy, Er) solid solutions. Journal of Alloys and Compounds, **282**(1-2), p. 101-108 (1999).
5. T.H. Okabe, M. Nakamura, T. Oishi, and K. Ono, Electrochemical deoxidation of titanium. Metallurgical Transactions B, **24**(3), p. 449-455 (1993).
6. G.Z. Chen, D.J. Fray, and T.W. Farthing, Direct electrochemical reduction of titanium dioxide to titanium in molten calcium chloride. Nature, **407**(6802), p. 361-364 (2000).
7. Y. Sakamura, M. Kurata, and T. Inoue, Electrochemical Reduction of UO_2 in Molten $CaCl_2$ or LiCl. Journal of the Electrochemical Society, **153**(3), p. D31-D39 (2006).
8. A.M. Abdelkader, A. Daher, R. Abdelkareem, and E. El-Kashif, Preparation of Zirconium Metal by the Electrochemical Reduction of Zirconium Oxide. Metallurgical and Materials Transactions B, **38**(1), p. 35-44 (2007).
9. A.M. Abdelkader and D.J. Fray, Electro-deoxidation of hafnium dioxide and niobia-doped hafnium dioxide in molten calcium chloride. Electrochimica Acta, **64**(0), p. 10-16 (2012).
10. B. Claux, J. Serp, and J. Fouletier, Electrochemical reduction of cerium oxide to metal. Electrochimica Acta, **56**(7), p. 2771-2780 (2011).
11. Z.F. Cai, Z.M. Zhang, Z.C. Guo, and H.Q. Tang, Direct electrochemical reduction of solid vanadium oxide to metal vanadium at low temperature in molten $CaCl_2$-NaCl. International Journal of Minerals Metallurgy and Materials, **19**(6), p. 499-505 (2012).
12. C.Z. George, G. Elena, and J.F. Derek, Direct electrolytic preparation of chromium powder. Metallurgical and Materials Transactions B, **35**(2), p. 223-233 (2004).
13. E.Y. Choi, J.M. Hur, I.K. Choi, S.G. Kwon, D.S. Kang, S.S. Hong, H.S. Shin, M.A. Yoo, and S.M. Jeong, Electrochemical reduction of porous 17 kg uranium oxide pellets by selection of an optimal cathode/anode surface area ratio. Journal of Nuclear Materials, **418**(1-3), p. 87-92 (2011).
14. G.M. Haarberg, Electrodeoxidation of solid Fe_2O_3 in molten $CaCl_2$ to produce iron, in 8th International Conference on 'molten slags, fluxes and salts': Santiago, Chile(2009).
15. J.J.-Y. SANG MUN JEONG, SEO Chung-Seok, PARK Seong-Won, Characteristics of an electrochemical reduction of Ta_2O_5 for the preparation of metallic tantalum in a LiCl-Li_2O molten salt. Journal of Alloys and Compounds, p. 210-215 (2007).
16. M. Iizuka, T. Inoue, M. Ougier, and J.P. Glatz, Electrochemical reduction of (U,PU)O_2 in molten LiCl and $CaCl_2$ electrolytes. Journal of Nuclear Science and Technology, **44**(5), p. 801-813 (2007).
17. H.W. Xie, H. Zhang, Y.C. Zhai, J.X. Wang, and C.D. Li, Al Preparation from Solid Al_2O_3 by Direct Electrochemical Deoxidation in Molten $CaCl_2$-NaCl at 550 ºC. Journal of Materials Science & Technology, **25**(4), p. 459-461 (2009).
18. T. Nohira, K. Yasuda, and Y. Ito, Pinpoint and bulk electrochemical reduction of insulating silicon dioxide to silicon. Nature Materials, **2**(6), p. 397-401 (2003).
19. K. Yasuda, T. Nohira, R. Hagiwara, and Y.H. Ogata, Direct electrolytic reduction of solid SiO_2 in molten $CaCl_2$ for the production of solar grade silicon. Electrochimica Acta, **53**(1), p. 106-110 (2007).
20. R. Abdulaziza, L.D. Browna, D. Inman, S.J.R. Simonsa, P.R. Shearinga, and D.J.L. Bretta, A Fluidised Cathode Process for the Electrochemical Reduction of Tungsten Oxide in A Molten LiCl-KCl Eutectic. Ecs Journal of Solid State Science and Technology, **58**(19), p. 65-74 (2014).
21. R. Bhagat, M. Jackson, D. Inman, and R. Dashwood, The Production of Ti–Mo Alloys from Mixed Oxide Precursors via the FFC Cambridge Process. Journal of electrochemical society, **155**(6), p. E63-E69 (2008).

22. R. Bhagat, M. Jackson, D. Inman, and R. Dashwood, Production of Ti-W Alloys from Mixed Oxide Precursors via the FFC Cambridge Process. Journal of the Electrochemical Society, **156**(1), p. E1-E7 (2009).
23. J.H. Du, Z.P. Xi, Q.Y. Li, Z.X. Li, and Y. Tang, Preparation of TiFe Alloy by Electro-Deoxidization in Molten Salt. Rare Metal Materials and Engineering, **37**(12), p. 2240-2243 (2008).
24. B. Jacksona, M. Jacksonb, D. Dyea, D. Inmana, and R. Dashwood, Production of NiTi via the FFC Cambridge Process. Journal of the Electrochemical Society, **155**(12), p. E171-E177 (2008).
25. F. Meng and H. Lu, Direct Electrochemical Preparation of NbSi Alloys from Mixed Oxide Preform Precursors. Advanced Engineering Materials, **11**(3), p. 198-201 (2009).
26. M. Gibilaro, J. Pivato, L. Cassayre, L. Massot, P. Chamelot, and P. Taxil, Direct electroreduction of oxides in molten fluoride salts. Electrochimica Acta, **56**(15), p. 5410-5415 (2011).
27. S. Seetharaman, ed. Fundamentals of metallurgy. 2005, Woodhead Publishing Limited: Cambridge.
28. A. Roine, In HSC Chemistry. Outotec Oyj Research: Espoo, Finland(2008).
29. O.A. T. Heumann, J. Less-Common Met, **6**, p. 108-117 (1964).
30. H. Iwasaki, O. Nittono, and Y. Koyama, CRYSTALLOGRAPHIC STUDY OF THE MARTENSITIC TRANSFORMATION IN INDIUM-TIN ALLOYS. Nippon Kinzoku Gakkai-si, **45**(7), p. 667-675 (1981).
31. T.B. Massalski, ed. Binary Alloy Phase Diagrams Second Edition Plus Updates. 1996, The Materials Information Society.
32. T. Studnitzky and R. Schmid-Fetzer, Phase formation and reaction kinetics in M–Sn systems (M = Zr, Hf, Nb, Ta, Mo). Zeitschrift für Metallkunde, **93**(9), p. 894-903 (2002).
33. B. Qin, P. Cui, A.M. Martinez, R.E. Aune, and G.M. Haarberg, Direct Electroreduction of Indium and Tin Oxides in Molten Salts. Molten Salts and Ionic Liquids 19, **64**(4), p. 249-255 (2014).
34. Y. Castrillejo, M.A. Garcia, E. Barrado, P. Pasquier, and G. Picard, Chemical and Electrochemical-Behavior of Indium Ions in the $ZnCl_2$-2NaCl Melt at 450 °C. Electrochimica Acta, **40**(17), p. 2731-2738 (1995).
35. J. Dutkiewicz and W. Zakulski, eds. Alloy Phase Diagrams. Vol. 5. 1984.
36. Z. Moser, J. Dutkiewicz, W. Gasior, and J. Salawa., eds. Alloy Phase Diagrams. Vol. 6. 1985.
37. J.C. Gabriel, J. Bouteillon, J.C. Poignet, and J.M. Roman, Electrochemistry of Molybdenum Solutions in Molten Licl-Kcl Eutectic at 500°C. Journal of the Electrochemical Society, **141**(9), p. 2286-2291 (1994).

Brief introduction

Bo Qin, PhD candidate, E-mail: qinboxingfu@126.com
Geir Martin Haarberg, corresponding author, E-mail: geir.martin.haarberg@ntnu.no